Serial block face scanning electron microscopy reveals novel organizational details of the retinal pigment epithelium

J. Arjuna Ratnayaka*, Eloise Keeling

Advances in imaging have led to the development of several new types of microscopes such as serial block face scanning electron microscopy (SBF-SEM), lightsheet microscopy, as well as X-ray micro-computed tomography (micro-CT), which enables the study of samples in fundamentally different ways. Significantly, these are now commercially available, which facilitates their widespread use in research. With SBF-SEM, fixed and resin-embedded specimens can be serially sectioned and imaged to construct a 3D dataset of the ultrastructure of cells and tissues at high resolution. We used this technique on perfusion-fixed C57BL/6 mouse eyes to image the outer retina. Our findings revealed novel organizational details of the retinal pigment epithelium (RPE) (Keeling et al., 2020b); a specialized cell monolayer that maintains the overlying photoreceptors and also forms the outer blood-retinal-barrier. RPE cells were found to look after far more photoreceptors than was widely assumed. 3D-data enabled measurements of the RPE cytoplasmic and nuclear volumes, the length and angle of microvilli on the apical RPE surface, as well as sub-RPE spaces under the basolateral membrane. The study also compared between mono-nucleate vs. bi-nucleate RPE cells, whilst the use of computing microinstructions (macros) provided information on interactions between adjacent cells in the RPE monolayer. Analysis of SBF-SEM stacks showed several hundred mitochondria which were rendered in 3D, providing information on their volume and spatial distribution in healthy RPE. Mitochondria were found in varying shapes and sizes, and predominantly localized to the mid and basal-zones of cells. The capabilities of SBF-SEM alongside other imaging techniques are being increasingly harnessed by investigators to gain novel insights into the organization of cells and tissues in the eye. These findings also help improve the current understanding of pathology linked with common blinding conditions such as age-related macular degeneration (AMD), as well as rare forms of retinopathy which leads to irreversible sight-loss.

Studies of human donor eye tissues as well as animal and *in vitro* cell models show that pathogenic changes at the ultrastructural level can precede clinical symptoms by many years. These findings have largely come from the use of conventional light and electron microscopy (EM) methods, which has laid the foundation for our current understanding of how cells and tissues change with age, and how disease develops in the eye. Recent advances in EM and super-resolution microscopy have enabled investigators to push the boundaries of imaging even further, resulting in a plethora of exciting new findings. Some examples include studies that provide new insights into the organization of photoreceptors (Volland et al., 2015b), the dynamics of cone mitochondria in the zebrafish (Giarmarco et al., 2020) and remodeling of the RPE basal labyrinth (Hayes et al., 2019) as well as the composition of autofluorescent macromolecules in RPE cells (Bermond et al., 2020). In the past, considerations such the size and thickness of a sample as well as its opacity posed significant barriers to its study. Volumetric data could only be obtained manually by serial EM sections which was technically very demanding. Often compromises were made, where a single imaging parameter had to be prioritized to the detriment of others: for instance, favoring a higher magnification resulted in a diminished field of view. Although these tension points still feature in modern microscopy, investigators now have a range of options to mitigate such undesirable effects or circumvent them altogether. The recent introduction of tile-scans for instance on many of the instruments make detailed scrutiny of large fields of view a possibility. New techniques also allow the microscopist to exploit the advantages of light, EM and X-ray microscopy in obtaining a more holistic view of the sample. Approaches such as correlative light and electron microscopy enable studies to combine fluorescence readouts with high EM-resolution imaging. The incorporation of automation has promoted increased sophistication of serial studies and importantly, made it more accessible to investigators who are not specialists. SBF-SEM used in our work resulted in the destruction of the samples. However, if sectioned tissues are required for subsequent analysis, techniques such as array tomography can be used where serial ultrathin sections are collected on a solid substrate from which light and electron images can be acquired afterwards. However, for true non-destructive imaging, investigators can use approaches such as micro-CT.

In our recent work, we used SBF-SEM to investigate the architecture of healthy RPE cells from the central mouse retina (Keeling et al., 2020b). To our knowledge, the study was the first to fully reconstruct a section of the RPE monolayer in 3D. Our findings showed unidirectionally arranged microvilli of approximately 5.5 µm in length on the apical RPE surface (**Figure 1A**). The height of RPE cells including microvilli was ~12 m, which was broadly similar to values reported in humans. These microvilli were angled at ~143.0° and intimately associated with the outer segments of overlying photoreceptors. Footprints of the outer segments could be observed on the microvilli bed, indicating where the distal ends of photoreceptors terminated (Keeling et al., 2020b). We speculate that the unidirectional organization of microvilli could help optimize RPE-photoreceptor interactions. Closer examination of 3D-reconstructed images reveals that RPE microvilli associate intimately with any accessible surface of outer segments (**Figure 1B** and **C**). When considered from a 3D perspective, it appears that microvilli are present around as well as in-between single or clusters of outer segments to maximize this interaction. The extent of this association can be fully appreciated by viewing a supplementary movie of a SBF-SEM stack published in the original research article (Keeling et al., 2020b). Conventional EM studies have shown how the orderly arrangement of outer segments becomes disrupted with retinopathy. 3D-imaging can be used in the future to gain a more detailed understanding of this phenomenon. An important finding was that RPE cells maintained far more photoreceptors than had been previously thought. 3D-imaging revealed that each RPE cell interacted with 90–216 photoreceptors (Keeling et al., 2020b). This is in contrast to conventional EM studies carried out in the rhesus monkey retina that showed each RPE supporting between 39–45 photoreceptors (Young, 1971). Our data was also consistent with a previous report which used standard EM approaches that showed high numbers of photoreceptors interacting with RPE in the mouse retina (Volland et al., 2015a). Taken together, these findings can have important implications for assessing the risk of retinopathy, as the proteolytic burden of healthy RPE cells may have been considerably underestimated. The daily internalization of outer segments and their subsequent degradation by RPE cells is an important function of this monolayer, as deficiencies in these mechanisms result in the accumulation of incompletely degraded intracellular material. These aggregates, termed lipofuscin and its derivatives, are thought to contribute to autofluorescence in RPE cells, a characteristic feature of this monolayer. For example, lipofuscin accounts for ~20% of the RPE cytoplasm by the eighth decade of life. Outer segments may also be subject to photo-oxidative modifications before internalization as well as further modifications once inside RPE cells. Although recent findings in patients suggests that lipofuscin and its autofluorescent signal

becomes stable or even declines with AMD, numerous studies have shown the pathogenic effects of oxidatively modified outer segments as well as bisretinoid fluorophores in RPE cells (Sparrow et al., 2012; Keeling et al., 2020a). The excessive build-up of lipofuscin however, is correlated with RPE atrophy, as demonstrated in patients carrying mutations in the *ABCA4* gene. We have provided a supporting link that allows readers to 3D-print an entire RPE cell from our data, which can be a useful tool for teaching (**Additional file 1**).

Our study also compared mono-nucleate *vs*. bi-nucleate RPE in the central mouse retina. The murine retina contains high levels of bi-nucleate RPE cells compared to the human equivalent. However, direct comparisons between multinucleation in the human and rodent RPE may not be accurate given the important differences between these species such as the lack of an anatomical macula in rodents. Nonetheless, RPE multinucleation is linked with oxidative stress, impaired autophagy as well as loss of contact with overlying photoreceptors. We anticipate that future 3D-imaging studies will enable a more in-depth scrutiny of these processes. Interestingly, our study revealed that nuclear dimensions were largely consistent, irrespective of their number, in each RPE cell (Keeling et al., 2020b). An important observation was that when nuclear volumes were excluded, the cytoplasmic volumes of bi-nucleate and mono-nucleate RPE were broadly similar. Another observation was that bi-nucleate RPE maintained more photoreceptors; an average of 139.5 photoreceptors per cell which includes some incompletely 3D-rendered RPE *vs*. 90 photoreceptors in mono-nucleate RPE. Although further studies are required to verify this, our findings suggest that compared to RPE with a single nucleus, bi-nucleate RPE cells may be susceptible to a higher proteolytic burden. Our *a priori* hypothesis is consistent with the association of multinucleation with aforementioned disease processes, including sub-RPE drusen (Al-Hussaini et al., 2009). The accumulation of sub-RPE proteins/lipids in the macula is linked with an increased likelihood of AMD. Our observation that these cells also contained more sub-RPE spaces compared to mono-nucleate RPE (Keeling et al., 2020b) also supports an association of bi-nucleate RPE with disease. Another study, which also used SBF-SEM, showed loss of the RPE basolateral labyrinth with age and disease (Hayes et al., 2019). Loss of palisade-like structures and disorganized basolateral infolds have been reported in donor human tissues and in rodent models of retinal degeneration. 3D-approaches could be used to further scrutinize any correlation between bi-nucleate RPE cells and retinopathy.

The RPE monolayer in the human eye is thought to contain 4.2–6.1 million cells and is organized such that they have a cobblestone-like appearance. Although RPE cells are often depicted adopting a hexagonal shape, 2D analysis of RPE flatmounts and 3D-reconstructions from the mouse central retina shows pentagonal as well as cuboidal shaped cells (Keeling et al., 2020b). An important function of the RPE monolayer is the formation of a barrier delineating the retinal space from the systemic environment. Integral to this is the bond between adjacent RPE that are formed by apical junctional complexes which encircles each cell and consists of adherens and tight junctions as well as, unusually, gap junctions. Whilst the resolution of SBF-SEM images did not allow the visualization of these complexes, cross-sectional views of 3D-reconstructed RPE revealed that cells adopted a rhomboid rather than a columnar or cuboidal shape. As a rhomboid creates a larger cross-sectional interface compared to a rectangle or square, we speculate that such an arrangement may be an adaptation to increase cell-cell contact between adjacent RPE in the monolayer. A macro developed to measure the interface between RPE, reported a surface area of ~48 μm^2 between adjacent cells (Keeling et al., 2020b). The breakdown of junctional complexes in disease is likely to be accompanied by a diminishing area of contact between cells, which can be quantified in a similar fashion. An example of such pathology is the neovascular form of AMD, where an impaired blood-retinal-barrier is associated with increased paracellular permeability, followed by migration of myeloid cells from systemic circulation, neovascularization as well as inflammation in later stages of the disease.

SBF-SEM datasets also showed the presence of mitochondria that were identified by their shapes and sizes as well as the presence of cristae. This method of identification allowed the 3D-reconstruction of mitochondria in a sub-set of RPE cells. Conventional EM studies in RPE cells of the rhesus monkey had previously shown how mitochondrial numbers decreased whilst their length increased with age (Gouras et al., 2016). Our 3D dataset indicated a heterogeneous mitochondrial population in healthy RPE (Keeling et al., 2020b) and revealed details of their structure as well as spatial distribution. The combined volume of mitochondria made up 11.5% of the total RPE cytoplasm. A total number of 422 mitochondria were identified in the mono-nucleate RPE cell compared to 678 mitochondria in the bi-nucleate RPE cell. Another study using a similar approach reported 198 mitochondria in a neuron from the mouse brain. In order to analyze the distribution of mitochondria in RPE cells, we horizontally sectioned each cell (virtually from the dataset) along its apical-basal axis, which revealed the apical-zone of RPE to contain the least number of mitochondria. The mid-zone of the mono-nucleate RPE cell contained the highest number as a percentage of the total mitochondrial population (**Figure 1D**). Mitochondria in the bi-nucleate RPE cell were evenly distributed between the mid and basal-zones (**Figure 1E**). Closer scrutiny of the mid-zone in both cells revealed significantly more mitochondria in the lower portion compared to the upper half. However, mitochondria in the bi-nucleate RPE appeared to be smaller, fragmented and more densely packed compared to the mono-nucleate cell. This may partly be due to the larger number of mitochondria in the bi-nucleate RPE that are packed into a 3D-cytoplasmic space which is broadly similar to a smaller mono-nucleate RPE cell. The overall mitochondrial distribution was somewhat different to that reported in the monkey, where the apical portion of RPE cells was almost devoid of any mitochondria, whilst the mid and basal-zones contained progressively larger numbers (Gouras et al., 2016). This discrepancy could be due to differences between conventional EM *vs*. SBF-SEM approaches, or variances between RPE with different numbers of nuclei. A further contributing factor may be the dynamic nature of mitochondria, which continuously fragment and reform through a processes of fission and fusion. The high photo-oxidative retinal environment, which predisposes damage to these organelles, coupled with the inability of post-mitotic RPE to repair any damage through cell division, means that impaired mitochondrial function is strongly associated with retinopathies such as AMD (Kaarniranta et al., 2020). Use of 3D-imaging has recently provided fascinating insights into the dynamic behaviors of mitochondria in zebrafish photoreceptors. Mitochondria were shown to undergo biogenesis at night resulting in an increasing number of smaller, simpler organelles and elevated metabolic activity in cones. By contrast, during daylight, an association with the endoplasmic reticulum and autophagosomes led to a decrease in mitochondrial numbers (Giarmarco et al., 2020). Their study also showed large, green cone photoreceptors to contain > 700 mitochondria with 300–450 mitochondria in smaller green cone cells. Furthermore, large mega-mitochondria were reported in zebrafish photoreceptors, which we did not observe in RPE cells from the central mouse retina. Given the high metabolic demands of photoreceptors, the large numbers of mitochondria in these cells were unsurprising. Nonetheless the elaborate circadian-related changes provide novel insights into how mitochondrial structure and function may be regulated to optimize vision in zebrafish. SBF-SEM could be similarly used to investigate whether mitochondria are re-organized in RPE cells in response to changing metabolic requirements and disease. Such strategic arrangement of mitochondria is a well-characterized feature in axons, which can span up to a meter in length. Disruption to the anterograde and retrograde movements of mitochondria, longer spacing between mitochondria, or axonal segments that are devoid of mitochondria, leads to deficiencies in Ca^{2+} homeostasis, lipid biosynthesis as well as lack of ATP amongst other features,

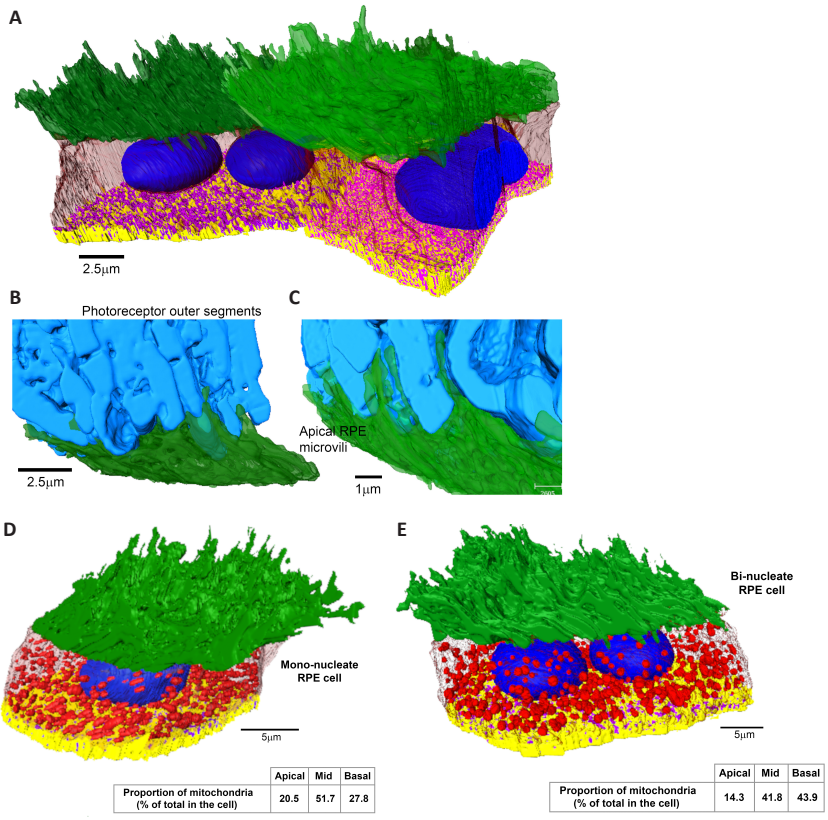

	Apical	Mid	Basal
Proportion of mitochondria (% of total in the cell)	20.5	51.7	27.8

	Apical	Mid	Basal
Proportion of mitochondria (% of total in the cell)	14.3	41.8	43.9

Figure 1 | **3D-architecture of cells in the retinal pigment epithelium (RPE), interactions with photoreceptor outer segments and 3D-distribution of mitochondria in RPE cells.**
(A) A reconstructed section of the RPE monolayer showing mono-nucleate and bi-nucleate cells. Apical microvilli (green), cell cytoplasm (transparent), nuclei (blue) basolateral membrane (yellow) with sub-RPE spaces created by basolateral infolds (purple). Note, the unidirectional arrangement of apical microvilli. Scale bar: 2.5 µm. (B, C) Apical microvilli (green) of two separate 3D-reconstructed RPE cells can be observed to associate intimately with photoreceptor outer segments (light blue). Note, the extent of this association, where RPE microvilli project in-between as well as around outer segments. Scale bars in B and C: 2.5 µm and 1 µm, respectively. (D) Mono-nucleate and (E) bi-nucleate RPE cells highlighting the shapes, sizes as well as the spread of mitochondria. The proportion of mitochondria along the apical-basal axis in each third of the cell was calculated, which revealed these organelles to be predominantly localized to the mid and basal-zones. Apical microvilli (green), cell cytoplasm (transparent), nuclei (blue), mitochondria (red), basolateral membrane (yellow) with sub-RPE spaces created by basolateral infolds (purple). Scale bars: 5 µm. Unpublished data.

which indicate early neuropathology. Similar mis-localization of mitochondria has been reported in the soma and dendrites of motor neurons and in spinal cord sections from patients with amyotrophic lateral sclerosis.

Recent advances in microscopy have ushered in a renaissance in imaging, enabling the study of ocular anatomy in previously unprecedented ways. When combined with the rapidly evolving field of non-invasive retinal imaging, which includes spectral domain optical coherence tomography and microperimetry, these offer the tantalizing prospect of providing further insights into ageing as well as disease-linked changes in the retina. Increasing accessibility of these technologies are likely to encourage studies that combine longitudinal assessments of living eyes with analyses of well-preserved retinal tissues, allowing a better correlation of disease with ultrastructural changes at the cellular and tissue level. In the longer-term, such insights can help pave the way for developing effective new treatments for conditions that cause irreversible sight-loss.

We are grateful to Dr David S. Chatelet for help with the reconstruction and analysis of 3D images, and to Dr Anton Page for scrutinizing the manuscript. Drs Chatelet and Page are at the Biomedical Imaging Unit, University of Southampton, UK.

The present work was supported by the Awards to JAR from the UK Macular Society, UKRI Quality Research Strategic Priorities Fund from Public Policy Southampton (New Things Fund) as well as the Gift of Sight Appeal.

J. Arjuna Ratnayaka*, Eloise Keeling
Clinical and Experimental Sciences, Faculty of Medicine, University of Southampton, Southampton, UK
***Correspondence to:** J. Arjuna Ratnayaka, PhD, J.Ratnayaka@soton.ac.uk.
https://orcid.org/0000-0002-1027-6938 (J. Arjuna Ratnayaka)
https://orcid.org/0000-0003-0399-359X (Eloise Keeling)
Date of submission: January 15, 2021
Date of decision: February 7, 2021
Date of acceptance: March 16, 2021
Date of web publication: August 4, 2021

https://doi.org/10.4103/1673-5374.321002
How to cite this article: *Ratnayaka JA, Keeling E (2022) Serial block face scanning electron microscopy reveals novel organizational details of the retinal pigment epithelium. Neural Regen Res 17(3):569-571.*

Additional file:
Additional file 1: *RPE cell for 3D-printing.*

References

Al-Hussaini H, Schneiders M, Lundh P, Jeffery G (2009) Drusen are associated with local and distant disruptions to human retinal pigment epithelium cells. Exp Eye Res 88:610-612.
Bermond K, Wobbe C, Tarau IS, Heintzmann R, Hillenkamp J, Curcio CA, Sloan KR, Ach T (2020) Autofluorescent granules of the human retinal pigment epithelium: phenotypes, intracellular distribution, and age-related topography. Invest Ophthalmol Vis Sci 61:35.
Giarmarco MM, Brock DC, Robbings BM, Cleghorn WM, Tsantilas KA, Kuch KC, Ge W, Rutter KM, Parker ED, Hurley JB, Brockerhoff SE (2020) Daily mitochondrial dynamics in cone photoreceptors. Proc Natl Acad Sci U S A 117:28816-28827.
Gouras P, Ivert L, Neuringer M, Nagasaki T (2016) Mitochondrial elongation in the macular RPE of aging monkeys, evidence of metabolic stress. Graefes Arch Clin Exp Ophthalmol 254:1221-1227.
Hayes MJ, Burgoyne T, Wavre-Shapton ST, Tolmachova T, Seabra MC, Futter CE (2019) Remodeling of the basal labyrinth of retinal pigment epithelial cells with osmotic challenge, age, and disease. Invest Ophthalmol Vis Sci 60:2515-2524.
Kaarniranta K, Uusitalo H, Blasiak J, Felszeghy S, Kannan R, Kauppinen A, Salminen A, Sinha D, Ferrington D (2020) Mechanisms of mitochondrial dysfunction and their impact on age-related macular degeneration. Prog Retin Eye Res 79:100858.
Keeling E, Culling AJ, Johnston DA, Chatelet DS, Page A, Tumbarello DA, Lotery AJ, Ratnayaka JA (2020a) An in-vitro cell model of intracellular protein aggregation provides insights into RPE stress associated with retinopathy. Int J Mol Sci 21:6647.
Keeling E, Chatelet DS, Tan NYT, Khan F, Richards R, Thisainathan T, Goggin P, Page A, Tumbarello DA, Lotery AJ, Ratnayaka JA (2020b) 3D-reconstructed retinal pigment epithelial cells provide insights into the anatomy of the outer retina. Int J Mol Sci 21:8408.
Sparrow JR, Gregory-Roberts E, Yamamoto K, Blonska A, Ghosh SK, Ueda K, Zhou J (2012) The bisretinoids of retinal pigment epithelium. Prog Retin Eye Res 31:121-135.
Volland S, Esteve-Rudd J, Hoo J, Yee C, Williams DS (2015a) A comparison of some organizational characteristics of the mouse central retina and the human macula. PLoS One 10:e0125631.
Volland S, Hughes LC, Kong C, Burgess BL, Linberg KA, Luna G, Zhou ZH, Fisher SK, Williams DS (2015b) Three-dimensional organization of nascent rod outer segment disk membranes. Proc Natl Acad Sci U S A 112:14870-14875.
Young RW (1971) The renewal of rod and cone outer segments in the rhesus monkey. J Cell Biol 49:303-318.

C-Editors: Zhao M, Qiu Y; T-Editor: Jia Y